DOI: 10.1002/ejoc.200901435

Preparation and Conformation Analysis of *N*-(Ferrocenoyl)dipeptide Esters and Their 1′-Acetyl Derivatives

Jasmina Lapić,[a] Senka Djaković,[a] Ivan Kodrin,[b] Zlatko Mihalić,[b] Mario Cetina,*[c][‡] and Vladimir Rapić*[a]

Keywords: Bioorganometallic chemistry / Conformation analysis / Ferrocene / Peptides / Hydrogen bonds / Pi interactions / Density functional calculations

Ferrocene-containing dipeptides X-Fn-CO-AA-AA-OMe (**3/4**, X = H, AA = Gly/Ala; **5/6**, X = Ac, AA = Gly/Ala, Fn = ferrocene-1,1′-diyl) were prepared in 51–67 % yields from the starting appropriate ferrocenecarboxylic acid and dipeptide ester by the HOBt/EDC protocol. Conformation analysis of these bioconjugates was performed by spectroscopic methods (IR, ^{1}H and ^{13}C NMR, CD) and by X-ray crystal structure analysis, as well as by molecular modelling (DFT). Crystallographic analysis showed that self-assembly processes prevailed in compound **5**, and almost exclusively hydrogen-bonded species were also detected in all the compounds studied in the solid state by IR spectroscopy (KBr). Spectroscopic studies of conjugates **3**–**6** undertaken in solution in nonpolar solvents demonstrated formation of intra- and interchain weak to medium hydrogen bonds spanning NH_{AA2} with 1-FcCO, 1′-FcCO and/or N_{AA1} (Fc = ferrocenyl). The same experiments revealed that NH_{AA1} is not involved in hydrogen bonds. The interchain hydrogen bond in conjugate **6** caused a (*P*)-helical arrangement of the ferrocene moiety exhibiting a positive Cotton effect at 495 nm (246 deg M^{-1} cm^{-1}). All of the experimental findings were corroborated by DFT calculations, which furthermore showed conformation preferences in respect to the natural amino acid side chain of conjugates **3**–**6**.

Introduction[1]

Turns are ubiquitous elements in the secondary structures of proteins. Understanding and control of secondary structures of proteins, peptides and oligoamides is fundamentally important for the design of functional peptidic materials[2–5] in, for example, the field of molecular machines.[6] The use of molecular templates (scaffolds) is a widely exploited strategy in these studies.[7] These scaffolds nucleate or propagate a certain conformation from their ordered region through a substructure portion consisting of natural amino acids to form α-helices or β-sheet structures. In this context, 1,1′-disubstituted ferrocene conjugates with amino acids or short peptides have been successfully used as redox-active scaffolds with an ideal distance between cyclopentadienyl rings (ca. 3.3 Å) to form turn elements based on intramolecular hydrogen bonding (IHB) interactions.[7,8] Symmetrically substituted bioconjugates of ferrocene-1,1′-dicarboxylic acid (Fcd) with one or two amino acids per substituent have been extensively studied. The majority of these compounds (independently of the number and type of the amino acid incorporated) form two intramolecular hydrogen bonds in the solid state. This results in the formation of two 10-membered rings (β-turn-like "Herrick conformation"). Usually, these intramolecular hydrogen bonds are sufficiently strong for this C_2-symmetrical conformation to be retained in chloroform solution.[9–19]

As a result of their constitutions, type **I** conjugates can form only *parallel* peptide strands (Scheme 1). The first symmetrical bioconjugates of 1,1′-diaminoferrocene were reported by Kraatz et al. (Scheme 1, type **II**).[20] In symmetrical ferrocene bioconjugates, two intramolecular hydrogen bonds are simultaneously formed between two amino acid substituents at two cyclopentadienyl rings. The situation is more complicated in asymmetric conjugates with only one amino acid substituent attached to one cyclopentadienyl ring (Scheme 1, types **III** and **IV**). The variants of type **III** (*n* = 1; X = OMe, NHMe; Y = Me, NHMe; R = H, Me, *i*Pr) have been investigated by us by a combination of experimental and theoretical methods (CD, IR and NMR spec-

[a] Department of Chemistry and Biochemistry, Faculty of Food Technology and Biotechnology, University of Zagreb, Pierottijeva 6, 10000 Zagreb, Croatia
Fax: +385-1-4836083
E-mail: vrapic@pbf.hr
[b] Department of Chemistry, Faculty of Science, University of Zagreb, Horvatovac 102A, 10000 Zagreb, Croatia
Fax: +385-1-4606401
E-mail: mihalic@chem.pmf.hr
[c] Department of Applied Chemistry, Faculty of Textile Technology, University of Zagreb, Prilaz baruna Filipovića 28a, 10000 Zagreb, Croatia
Fax: +385-1-3712599
E-mail: mcetina@ttf.hr
[‡] Corresponding author for X-ray analysis.
Supporting information for this article is available on the WWW under http://dx.doi.org/10.1002/ejoc.200901435.

troscopic techniques in combination with DFT calculations). We found that these conjugates in solution are best described as ensembles of conformers each featuring a single IHB. However, some conformations are significantly preferred over the others in solution.[21,22] In our recent study on "desymmetrized" 1,1′-diaminoferrocene conjugates of α-amino acids of type **IV** [R = H, Me (D- and L-Ala), *i*Pr] (Scheme 1) we showed that in weakly coordinating solvents, as well as in DMSO solution, they form a set of conformations with intramolecular hydrogen bonds involving the NH groups closest to the ferrocene unit.[23] The majority of the low-energy conformations possess a (*P*)-helical ferrocene chromophore for L-amino acid substituents, so chirality organization is already achieved through the attachment of one amino acid substituent at the 1,1′-diaminoferrocene central unit. The average strength of intramolecular hydrogen bonds in the investigated subset of compounds as estimated from ^{1}H NMR variation ratio values[21,24,25] is almost independent of the amino acid employed (i.e., the steric demand of the amino acid side chain R).

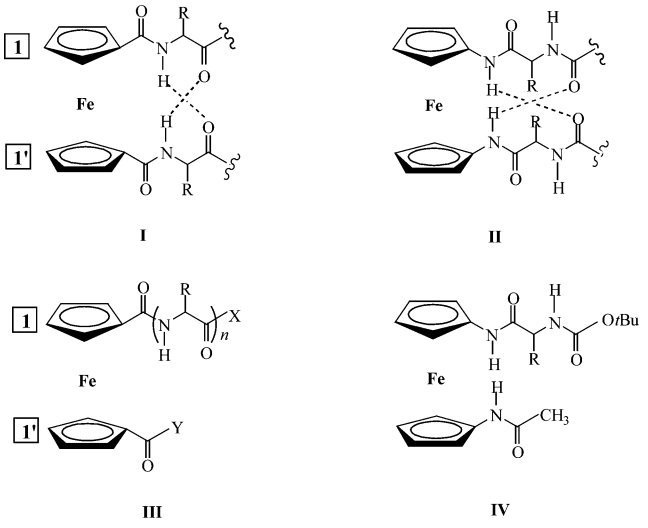

Scheme 1. Ferrocene-containing double-strand oligoamides (**I** and **II**) and their "desymmetrized" derivatives (**III** and **IV**).

Here our endeavours have been directed towards explaining the folding and conformation preferences of the desymmetrized conjugates of type **III** (*n* = 2; X = OMe; Y = Me; R = H, Me). With the abundance of conformations in subclass **III** (as well as in the case of type **IV**) as described in our previous papers[21,23] in mind, we decided here to reduce the number of NH groups (as IHB-donating functions), expecting smaller numbers of contributing conformations (i.e., more reliable conformation analysis). To address the question of individual conformation preferences in solution and to establish the molecular structure in the solid state we used spectroscopic methods (NMR, IR and CD) and X-ray crystal structural analysis, as well as DFT calculations.

Results and Discussion

Synthesis

The syntheses of esters **3**–**6** are depicted in Scheme 2. The starting compounds – ferrocenecarboxylic acid (**1**) and 1′-acetylferrocene-1-carboxylic acid (**2**) – were prepared by the procedures described previously.[26] Activation of these compounds with HOBt/EDC [HOBt = 1-hydroxybenzotriazole, EDC = *N*-(3-dimethylaminopropyl)-*N*′-ethylcarbodiimide hydrochloride] in CH_2Cl_2 and coupling with AA-AA-OMe (obtained from AA-AA-OMe·HCl by treatment with NEt_3) resulted in the formation of the *N*-(ferrocenoyl)dipeptide esters **3** and **4** and the *N*-(1′-acetylferrocenoyl)dipeptide esters **5** and **6** in yields of 51–67%.

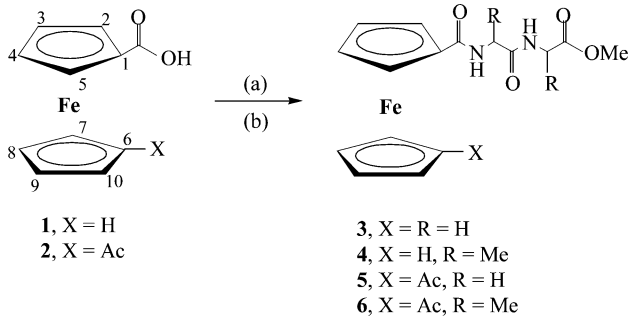

Scheme 2. Synthesis of Fc-CO-$(AA)_2$-OMe (**3** and **4**) and Ac-Fn-CO-$(AA)_2$-OMe (**5** and **6**). a) 1. HOBt/EDC, CH_2Cl_2; b) $(AA)_2$-OMe·HCl, NEt_3, CH_2Cl_2.

X-ray Crystal Structure Analysis

In **5** (Figure 1), the glycylglycine methyl ester moiety and the acetyl group are linked to the cyclopentadienyl (Cp) rings. The acetyl group is almost parallel to a C6–C10 ring. The dihedral angle between the atoms C17/O5/C18 and the mean plane of the ring is 4.54(19)°. The C11/N1/O1 atoms of the dipeptide moiety are slightly twisted out from the mean plane of the C1–C5 atoms and perpendicular with respect to the mean plane of the C12/C13/O2/N2/C14 atoms, as defined by the dihedral angles of 11.24(18) and 81.66(18)°, respectively.

The conformation of the dipeptide moiety is locked by two intramolecular hydrogen bonds: N2···N1 and C14···O2 (Figure 1). Each intramolecular hydrogen bond gives rise to a five-membered ring, which can be described by graph-set notation as *S*(5).[27] No intramolecular hydrogen bond of N–H···O type between juxtaposed strands is found, as a result of the almost parallel alignment of the acetyl group and the C11/N1/O1/C12 atoms of the dipeptide moiety [dihedral angle is 10.9(2)°]. The bond lengths in the Gly-Gly-OMe moiety (see Table S1 in the Supporting Information) fit well within the range for similar ferrocene structures.[24,28–31] The exceptions are the bond lengths C12–C13, N2–C14 and C14–C15, which are slightly longer in some closely related structures [ca. 0.02–0.03 Å] in which methyl, benzyl, benzylthiomethyl or methylthioethyl groups

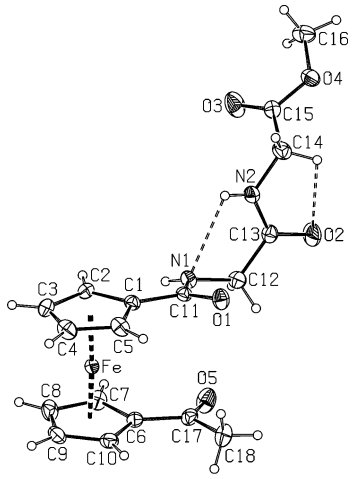

Figure 1. Molecular structure of **5**, with the atom numbering scheme; displacement ellipsoids for non-hydrogen atoms are drawn at the 30% probability level. The intramolecular hydrogen bonds are shown dashed.

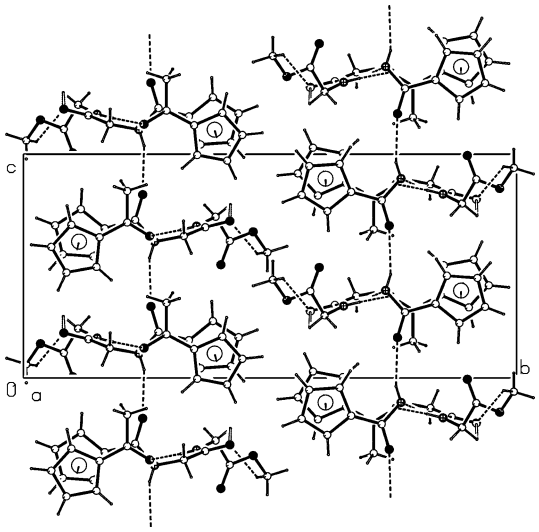

Figure 2. A crystal packing diagram of **5**, viewed along the *a* axis. Hydrogen bonds are indicated by dashed lines.

are attached to the C12 and C14 atoms. The carbonyl groups and Cp rings in **5** form an extended π-conjugated system, so the C1–C11 and C6–C17 bonds exhibit partial double bond character (Table S1 in the Supporting Information). The coplanar arrangement of a carbonyl group attached to the ring should allow maximum interaction of the two π-systems.[32]

The cyclopentadienyl rings are almost parallel to each other, with a tilt angle of 2.68(10)°. The conformation of the Cp rings is almost halfway between eclipsed and staggered. The values of the corresponding C–*Cg*–*Cg*–C pseudo-torsion angles, defined by joining two eclipsing Cp carbon atoms through the ring centroids (*Cg*), range from 15.43(14) to 15.72(12)°. This conformation could also be described by a torsion angle defined by the opposite Cp carbon atoms and the ring centroids, which for the fully eclipsed conformation would be 144° and for the staggered conformation would be 180°. The C1–*Cg*–*Cg*–C9 torsion angle in **5** is 159.71(13)°.

In the supramolecular aggregation of **5** both nitrogen atoms participate as proton donors (see Table S2 in the Supporting Information). The N1···O1^{i} hydrogen bond forms a characteristic $C(4)$[27] motif for structures possessing amide and carbonyl hydrogen-bonding functionalities, and links the molecules parallel to the *c* axis (Figure 2).

The N2···O5^{ii} hydrogen bond self-assembles the molecules into $C(10)$ chains parallel to the *a* axis (Figure 3). We have previously found that N–H···O hydrogen bonds generate both of these two chain motifs in closely related structures [$C(4)$ motif in Fc-CO-Ala-Phe-OMe[29] and Fc-CO-Cys(Bn)-Cys(Bn)-OMe;[30] $C(10)$ motif in Fn(CO-Ala-Phe-OMe)$_2$[29] and Fn(CO-Met-Met-OMe)$_2$[31]]. Only in the structure of Boc-Ala-Fca-Ala-Ala-OMe[28] does this hydrogen bond give rise to $C(11)$ chains. These two intermolecular N–H···O hydrogen bonds are augmented by one C–H···O hydrogen bond – C16···O2^{ii} (Table S2 in the Supporting Information) – that joins the molecules into $C(8)$ chains parallel to the *a* axis (Figure 3). The combination of the N2···O5^{ii} and C16···O2^{ii} hydrogen bonds gives rise to $R_2^2(16)$ rings. The supramolecular structure of **5** also contains weak aromatic π···π stacking interactions[33] between the Cp rings of neighbouring molecules (Figures 3 and 4).

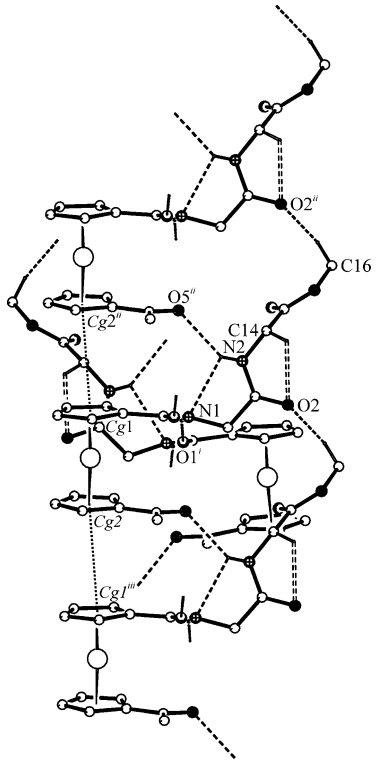

Figure 3. Part of the crystal structure of **5**, showing hydrogen bonds and aromatic π···π interactions (symmetry operators are given in Table S2 in the Supporting Information). For the sake of clarity, only hydrogen-bonding functionalities are shown. *Cg*1 and *Cg*2 are the centroids of rings C1–C5 and C6–C10, respectively. Hydrogen bonds and π···π interactions are indicated by dashed and dotted lines, respectively.

An interplanar angle between the rings is 2.67°, interplanar spacings are ca. 3.63 and 3.69 Å, a centroid separation is 3.9626(12) Å, and corresponding centroid–centroid offsets are ca. 1.45 and 1.60 Å, respectively. The π···π interactions do not give rise to a higher-dimensional supramolecular architecture because they link molecules in the same direction as the N2···O5^{ii} and C16···O2^{ii} hydrogen bonds. The two N–H···O hydrogen bonds, one C–H···O hydrogen bond and the aromatic π···π interactions in **5** thus give rise to a two-dimensional network (Figure 4).

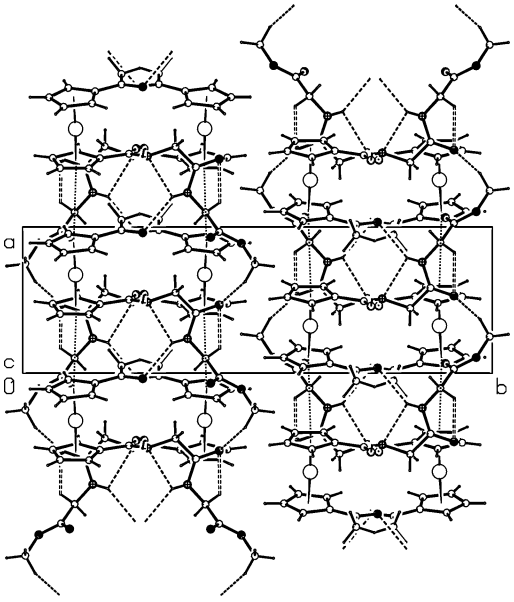

Figure 4. A crystal packing diagram of **5**, viewed along the *c* axis. Hydrogen bonds and π···π interactions are indicated by dashed and dotted lines, respectively.

Spectroscopic Analysis

As one can see from the previous section, crystal structure determination of the ester **5** showed that self-assembly processes prevail in the solid state. To establish the conformation preferences of the ferrocene-containing dipeptides **3**–**6** in CH_2Cl_2 and $CDCl_3$ (nonpolar solvents unable to act as hydrogen donors or acceptors), IR and ^{1}H NMR spectroscopic analysis was performed. To perform conformation analysis of *N*-(1′-acetylferrocenoyl)dipeptides **5** and **6** reliably we decided to compare their spectroscopic data with those for the monosubstituted *N*-(ferrocenoyl)dipeptides **3** and **4**. With the conformers of types **III** and **IV** compounds described in our recent papers in mind,[21,23] as well as the X-ray crystal structure data for compound **5**, possible N–H···O hydrogen bonding patterns in the related compounds studied are depicted in Scheme 3.

In the IR spectra of all the compounds investigated (CH_2Cl_2, $c = 10^{-2}$ M) signals ranging from 1742–1750 cm^{-1} ($\nu_{C=O}$, ester; Table 1) were found, indicating the absence of intrachain MeO–C=O···H–N bonds (that is, the **D** and **J** conformations do not contribute). The IR vibrations of the amino groups in **3** and **4** were registered at about 3430 and

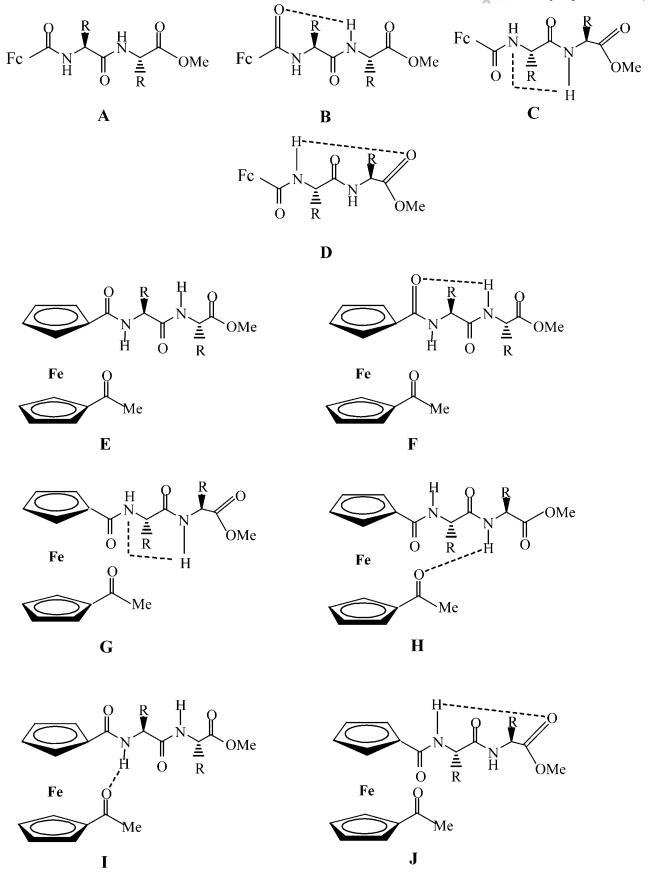

Scheme 3. Possible N–H···O hydrogen bond patterns in the model substances **3** and **4** (**A**–**D**; top) and in the *N*-(1′-acetylferrocenoyl)-dipeptides **5** and **6** (**E**–**J**; bottom).

3310 cm^{-1}, suggesting both free and hydrogen-bonded forms. Because the AA2 ester groups were not engaged in hydrogen bonding, one can assume conformations **B** (six-membered intramolecular hydrogen bonded ring involving FcC=O···H–N_{AA2}) and **C** (five-membered ring based on N_{AA1}···H–N_{AA2} IHB interactions), possibly accompanied by the open form **A**. IR spectra of the conjugates **5** and **6** in solution showed $\nu_{N-H\ free}$ at 3439/3425 and $\nu_{N-H\ assoc.}$ at 3347/3300 cm^{-1} (see Table 1). Because the NH frequencies in the spectra of all the compounds studied appeared at similar positions, analogously to the forms **A**–**C** proposed for **3** and **4**, the conformations **E**–**G** could be attributed to

Table 1. IR data [cm^{-1}] for **3**–**6** in CH_2Cl_2 ($c = 10^{-2}$ M) and in KBr.

		ν_{NH} (free)	ν_{NH} (assoc.)	ν_{CO} (ester)	ν_{CO} (amide I)	ν_{CO} (amide II)
3	CH_2Cl_2	3439 m	3323 w	1749 s	1682 s, 1660 s	1517 s
	KBr	–	3357 m, 3284 m	1719 s	1684 s, 1630 s	1544 s
4	CH_2Cl_2	3425 m	3309 w	1742 s	1682 s, 1650 s	1507 s
	KBr	3439 vw	3302 m	1748 s	1682 s, 1629 s	1540 s
5	CH_2Cl_2	3439 m	3347 mb	1750 s	1669 vs	1516 s
	KBr	–	3368 m, 3287 sh	1755 s	1649 vs	1517 s
6	CH_2Cl_2	3425 m	3330 mb	1742 s	1669 vs	1510 s
	KBr	3477 vw	3279 m	1743 s	1672 s, 1630 s	1550 s

the *N*-(acetylferrocenoyl)dipeptides **5** and **6**. Interchain NH hydrogen-bonded conformations **H** and **I** would be expected as well (Scheme 3).

The characters of the hydrogen bonds in the investigated compounds were investigated by IR dilution experiments, because the molecules should be unable to form intermolecular hydrogen bonds for stabilization in dilute solution. If, for example, the NH signal observed at 3347 cm^{-1} (at $c \approx 10^{-2}$ M) were to diminish and disappear on successive dilution to $c \approx 10^{-3}$ M, this would mean that this group was involved in an intermolecular hydrogen bond, whereas in the case that this frequency remained, that would be an indication of IHB. On dilution, the ratios of the free and associated NH frequencies in **3**–**6** as discussed above changed only a little in favour of those mentioned first, so one can assume intramolecular hydrogen bonds possibly accompanied (to a smaller extent) by self-association.

In the solid state (KBr), the absorptions of NH stretching vibrations in the spectra of conjugates **3**–**6** are found in the 3279–3368 cm^{-1} range, indicative of hydrogen-bonding interactions. Moreover, additional bands at 3439/3477 cm^{-1} appeared in the spectra of the alanine derivatives **4** and **6**, showing (similarly to the solution case) the presence of nonbonded NH functions too. In the dipeptides **4**–**6** in the solid state, the carbonyl groups belonging to the ester functions are observed at 1743–1755 cm^{-1}, suggesting that these subunits are not involved in hydrogen bonding. These data corroborate the X-ray crystal structure analysis findings for conjugate **5** on (intermolecularly) hydrogen-bonded amido groups and nonbonded ester carbonyl functions. An exception to this statement is to be found in the simplest molecule **3**, in which amido (3357, 3284 cm^{-1}) and possibly ester groups (1719 cm^{-1}) are also hydrogen-bonded (Table 1).

The NMR spectra of the conjugates **3**–**6** display the signals at their expected positions in accordance with the previously reported data for similar compounds.[21,24,28,34] As signments of proton and carbon chemical shifts (Table 2) were achieved by combined use of one- (^{1}H, APT) and two-dimensional NMR measurements (COSY, NOESY). In the ^{1}H NMR spectra amide protons are easily assigned on the basis of their distinct coupling patterns to the Hα protons of the amino acid side chain (i.e., doublets are observed for alanine derivatives **4** and **6** and triplets are found for glycine conjugates **3** and **5**).

It is worth mentioning that, to the best of our knowledge, no intrachain hydrogen-bonding interactions of the type **B/F** (γ-turn) have been described for the several so far published dipeptides Fc-CO-(AA)$_2$-OMe (AA = Gly, Ala, Phe, Pro).[13,17,29,31] [We first proposed (on the basis of thorough spectroscopic and theoretical analysis) the formation of such seven-membered intramolecularly hydrogen-bonded rings spanning FcCO and NHMe in amides MeNHCO-Fn-CO-AA-NHMe (AA = Gly, Ala, Val).[21]] As well as in the present X-ray analysis of conjugate **5**, the rather rare N···HN interaction (five-membered IHB rings, conformers **C** and **G**) was also found in our previous study on MeOOC-Fn-NHCO-Ala-Ala-OMe.[35] In a manner similar to that described for IR analysis, we also performed ^{1}H NMR dilution measurement experiments (Figure 5). Chemical shifts for NH_{AA2} protons in Gly (**5**) and Ala-dipeptide (**6**) did not change appreciably with successive reductions in concentration from $c = 1 \times 10^{-1}$ to 2.5×10^{-3} M. This weak dependence on concentration ($\Delta\delta \approx 0.4$ ppm) suggests medium (**5**, $\delta = 7.54$ ppm) and weak (**6**, $\delta = 7.14$ ppm) IHBs. The shift of the Gly1 signals for **5** from 7.01 to 6.4 ppm is an indication of very weak or no IHBs (or self-assembly processes) involving this NH group. The NH_{Ala1} resonance in conjugate **6** is only weakly dependent on concentration; if the very low chemical shift of this function ($\delta = 6.61$ ppm) is borne in mind, it is quite possible that this proton practically does not participate in HB. One has to stress that these

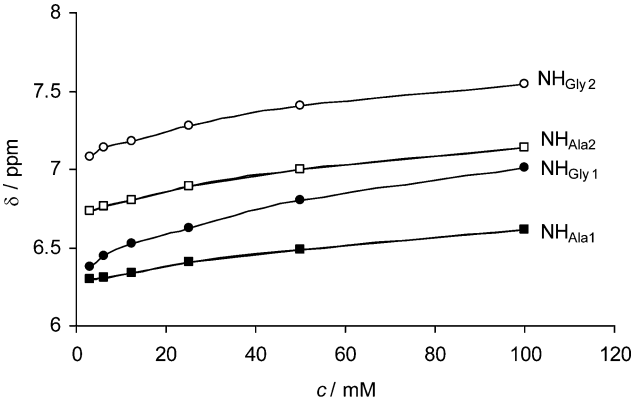

Figure 5. Concentration-dependent ^{1}H NMR chemical shifts of the amide protons of **5** and **6** in $CDCl_3$.

Table 2. Chemical shifts (δ), chemical shifts differences ($\Delta\delta$) and variation ratios (v.r.s) of the amide protons for dipeptides **3**–**6**, as well as δ and $\Delta\delta$ values for reference compounds **7**–**10**.

Compd.	Formula	δ ($CDCl_3$)[a]	δ ([D_6]DMSO)[a]	$\Delta\delta$	v.r. = $\Delta\delta$ substrate/$\Delta\delta$ reference (**ref. compd**.)
7	FcCOGlyOMe	6.28	8.24	1.96	
8	FcCOAlaOMe	6.22	8.07	1.85	
9	MeCOGlyOEt	6.08	8.25	2.17	
10	MeCOAlaOEt	6.02	8.23	2.21	
3	FcCOGlyGlyOMe	6.59, 6.89	8.27 8.07	1.68, 1.18	0.86 (**7**), 0.54 (**9**)
4	FcCOAlaAlaOMe	6.57, 7.22	7.71, 8.28	1.14, 1.06	0.62 (**8**), 0.48 (**10**)
5	AcFnCOGlyGlyOMe	7.01, 7.54	8.29, 8.20	1.28, 0.66	0.65 (**7**), 0.30 (**9**)
6	AcFnCOAlaAlaOMe	6.61, 7.14	7.80, 8.28	1.19, 1.14	0.64 (**8**), 0.52 (**10**)

[a] 1×10^{-1} M.

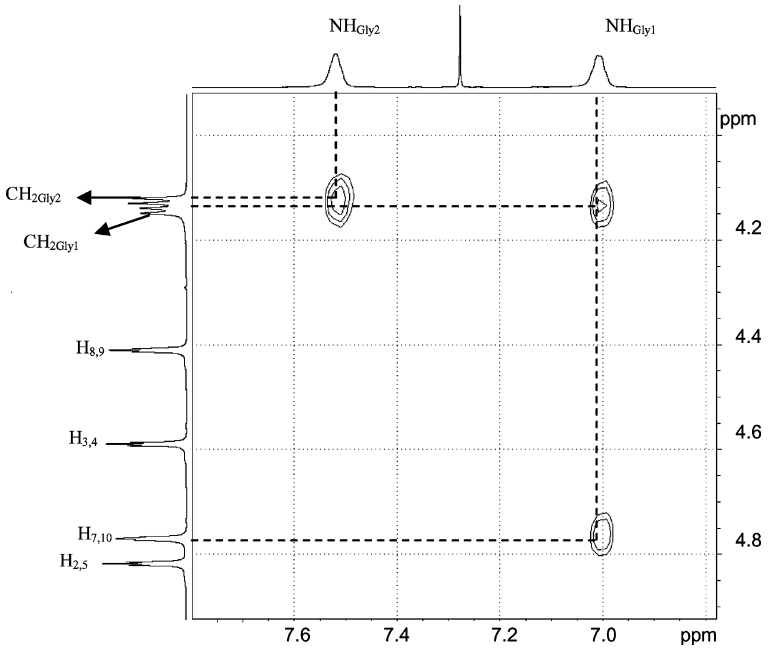

Figure 6. Part of the NOESY spectrum of **5**, indicating NOE contacts of NH protons with Cp–H and CH_2.

experiments gave information on the *stability or absence of hydrogen bonds involving specific NH groups, but tell us nothing about the conformation preferences.*

In the NOESY spectrum of compound **5** (Figure 6), NOE cross peaks from NH_{Gly1} to the cyclopentadienyl protons $H^{7,10}$ and CH_2 of the amino acid were observed, whereas NH_{Gly2} showed only contact with the adjacent CH_2, suggesting a 1,1′-arangement[36] of juxtaposed substituents.

Because the equilibrium between the contributing conformations is in general too fast for the NMR timescale, we do not observe separate signals for these forms (in contrast with the discrete IR bands characterizing free and associated molecules). Instead, average δ values between free and hydrogen-bonded species are observed. In this context one has to keep in mind that the position of equilibrium between intramolecular hydrogen-bonded and non-intramolecular hydrogen-bonded conformers is strongly solvent-dependent. Nonpolar solvents ($CHCl_3$, CH_2Cl_2) favour intramolecular hydrogen-bonded structures, whereas polar solvents such as DMSO (which acts as a strong HB-acceptor) disrupt hydrogen bonds to form solvates. Chemical shift differences ($\Delta\delta$) in $CDCl_3$ and [D_6]DMSO are measured to determine the strengths of specific hydrogen bonds (i.e. the stabilities of IHB rings): lower $\Delta\delta$ values mean stronger bonds and, vice versa, higher $\Delta\delta$ values are an indication of weaker ones.

To shed more light on the matter of the interactions of the investigated compounds with these solvents, it is very useful to perform [D_6]DMSO titrations with their $CDCl_3$ solutions.[37] Gradual addition of DMSO will typically cause a large change in chemical shift for free or weakly hydrogen-bonded amide NH protons, whereas tightly IHBd (intramolecularly hydrogen-bonded) NH functions trend to experience little or no effect from addition of this HB-accepting solvent. In other words, small downfield changes in chemical shift ($\Delta\delta \approx 0.6$ ppm) indicate IHBd species, whereas a significant change in chemical shift (>1 ppm) means that the NH under observation would not be expected to participate in IHB. Figure 7 shows the data from DMSO titrations of Gly-**5** and Ala-dipeptide **6**. The titration curves for all the NH protons (except NH_{Gly2}) are rather "steep" in the range from 0–25% [D_6]DMSO, with overall $\Delta\delta$ = 1.14–1.28 ppm. This is a strong indication of the absence of HB or weak hydrogen bond interactions with these functions. In contrast, for the NH_{Gly2} proton of conjugate **5**, $\Delta\delta$ = 0.66, meaning (consistently with our previous experiments) its participation in IHB of medium strength. Above ca. 25% DMSO the NH protons of all the compounds studied are in interaction with DMSO and this part of the titration is not very informative.

To address the position of the equilibrium between hydrogen-bonded and nonbonded states quantitatively – that is, to measure the populations of these forms – we compared them with *reference (standard) compounds* that cannot engage in hydrogen bonds. These reference compounds mimic the chemical environment about the NH groups in the ferrocenoylpeptides studied; appropriate reference compounds for the conjugate **5**, for example, are simple compounds **7** and **9** (Table 2), which can be considered "building blocks" for this conjugate. The ratio of the $\Delta\delta$ values for the ferrocene peptides and their reference compounds of each amide protons (the *variation ratio – v.r.*) is particularly useful for estimation of the extent to which the amide proton is engaged in IHB (v.r. = $\Delta\delta$ substrate/$\Delta\delta$ reference). In our previous publications on ferrocene-containing oligopeptides we found approximate relationships between v.r. range and IHB strength (stability of IHB rings) varying

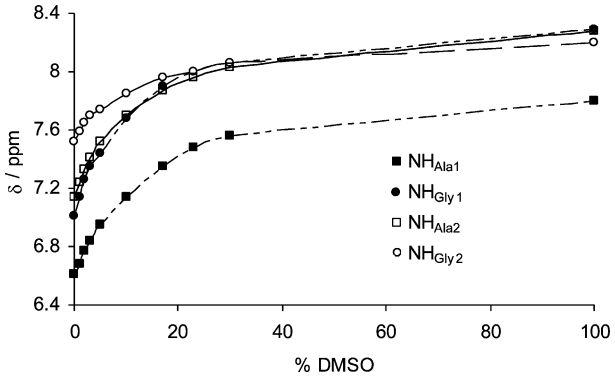

Figure 7. [D_6]DMSO titration of $CDCl_3$ solutions of the Gly conjugate **5** and the Ala dipeptide **6** showing chemical shift changes for NH_{AA2} and NH_{AA1}.

from zero (very strong intramolecular hydrogen bonds) to the values about 1 where there are no IHB interactions.[21,24]

In FcCOGlyGlyOMe (**3**) v.r.s of 0.86 and 0.54 (based on references **7** and **9**) were attributed to its NH_{Gly1} and NH_{Gly2} groups, indicating the absence of HB interactions and weak IHBs, respectively, in a more precise way (than by mere $\Delta\delta$ comparison); these data suggested that conformers **B** and/or **C** are present. We encountered a similar situation in the Ala analogue **4**: calculated v.r.s (by means of **8** and **10**) are 0.62 and 0.48, indicating (consistently with the IR data) free NH_{Ala1} and weakly IHBd NH_{Ala2}. Its 1′-Ac-substituted counterpart **6** showed similar v.r.s (0.64 for NH_{Ala1} and 0.52 for NH_{Ala2}). As well as the forms analogous to those proposed for conjugate **4** (**F** and **G**), the conformation population could be enriched here by **H** species. The situation of HB for NH_{Gly2} in conjugate **5** is somewhat different: its v.r. is significantly lower (0.30) than for its model compound **3** (0.65), indicating much stronger IHBs formed by intra- (**G**, **F**) and/or interchain (**H**) spanning by this group.

Participation of the form **H** in the conformation population of the alanine dipeptide **6** is additionally indicated by the important characteristic of its NMR spectra – the nonequivalence of protons and carbon atoms at positions 7/10 and 8/9. In other words, these pairs of atoms in the AcCp-ring are diastereotopic, due to intramolecular hydrogen bonds between CO-$(Ala)_2$-OMe and Ac subunits transferring chiral information from Ala moieties to the other Cp ring. A similar situation (as a consequence of efficient transmission across IHB) is found in AcNH-Fn-CO-(AA)-OMe,[38] but not in our previous study on MeOOC-Fn-$NHCO(Ala)_{1-2}$OMe.[35]

The prominent feature of peptides derived from $Fn(COOH)_2$- (**I**, **III**), $Fn(NH_2)_2$- (**II**, **IV**) and 1′-aminoferrocene-1-carboxylic acid (**Fca**) and containing chiral amino acids is helical chirality around the ferrocene moiety. In addition to crystallographic analysis in the solid state, CD spectroscopy is the method of choice for conformation analysis of these systems in solution. The compounds of types **I** and **II**, as well as **Fca** conjugates containing two or more L-amino acids, are characterized in the solid state by (*P*) helicity of the ferrocene unit, enforced by two strong intramolecular hydrogen bonds between the podand chains. Such conformations persist in solution in nonpolar solvents (CH_2Cl_2) and even in CH_3CN, showing excitation coupling signals around the UV/Vis absorption maxima at ca. 450 nm. Most of the described conjugates of types **I** and **II**, as well as their desymmetrized counterparts **III** and **IV** containing L-amino acids (see Scheme 1), showed positive Cotton effects shifted to lower energy. In the conjugates stabilized by two strong interchain hydrogen bonds (**I**, **II**, ...), addition of coordinating solvents (≈ 20% of DMSO) to their CH_2Cl_2 solutions leaves CD signals almost unchanged, indicating that the helicity of the ferrocene remains even in the presence of such hydrogen-bond-disrupting solvents. In the cases of compounds with weak or medium IHBs (**III**, **IV**), however, the formation of solvates overrides these intramolecular forces, which results in a significant reduction (or collapse) of the Cotton effect intensity.

The UV/Vis absorption band of Ac-Fn-CO-Ala-Ala-OMe (**6**) is observed at 455 nm. Its CD spectrum measured in CH_2Cl_2 ($c = 10^{-3}$ M) displays two maxima around this UV/Vis signal (at 428 and 495 nm; Figure 8). With the foregoing statement in mind, we considered that the second one (showing $M_\theta = 232$ deg M^{-1} cm^{-1}) should be decisive for the chiroptical properties of this conjugate. Consequently this compound should be characterized by (*P*) helicity, but the intensity of this signal is about one order of magnitude lower then those for type **I** (≈ 490 nm, M_θ ≈ 5000 deg M^{-1} cm^{-1}), once again indicating weak interchain hydrogen bonding. The instability of this IHB ring was demonstrated by addition of DMSO, on which as little as 2% of this HB-disrupting solvent caused a dramatic weakening of the CD signal. (N.B.: this phenomenon is consistent with the results of the NMR titrations presented in Figure 7). As would be expected, the CD spectrum of **6** measured in KBr (Figure S1 in the Supporting Information; absence of interchain HB), as well as the spectrum of FcCOAlaAlaOMe (**4**), showed almost flat curves ("CD silence") in the ferrocene chromophore region, clearly indicating that ferrocene chirality is responsible for this solvent-dependent Cotton effect.

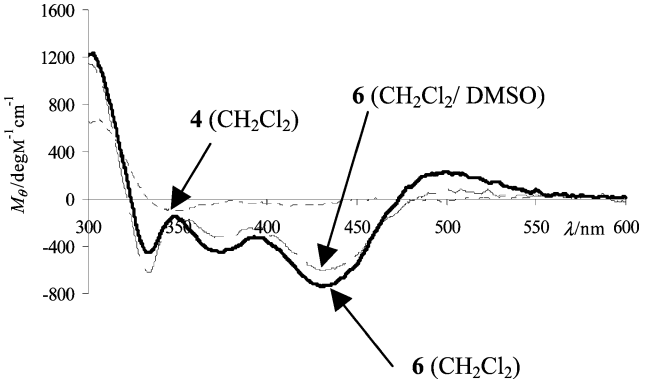

Figure 8. CD spectra of peptides **4** in CH_2Cl_2 and **6** in CH_2Cl_2 and CH_2Cl_2/DMSO (2% v/v).

Computational Study

DFT studies[21,23,35,38] have already proved useful for predicting distributions of disubstituted conformers, especially when hydrogen bonds are involved. For this paper we have performed complete conformation space searches for compounds **3**–**6** in chloroform solution. The number of NH groups was smaller than in the previously described type **III** substrates (Scheme 1),[21] thus making the analysis less computationally demanding.

Conformers can be classified on the basis of several common structural characteristics – ferrocene moiety geometry, number and type of intramolecular interactions and relative orientation of carbonyl groups. The orientations of the pairs of substituents of the disubstituted compounds **5** and **6** are designated by use of the 1,*n*′ convention and *E*/*Z* descriptors, whereas ferrocene helicity was designated by (*P*)- and (*M*)-symbols.[36]

The relative energies of the most stable conformers of monosubstituted (**3** and **4**) and disubstituted ferrocenes (**5** and **6**) in chloroform calculated at the B3LYP/6–311G(d,p)-LanL2DZ (& IEF-PCM) level of theory are given in Table 3 and their geometries in Figures 9 and 10.

For ferrocenoyldipeptides **3** and **4**, in addition to conformers without N–H···O hydrogen bonds (type **A**), one can predict the existence of **B**–**D**-type conformers possessing intrachain HBs (Scheme 3). The calculations showed that the **B** pattern with IHBd seven-membered ring is observed in more than two thirds of the population of ester **3**. The specific conformers (**3B1** and **3B2**) differ in the orientation of the substituent relative to the ferrocene moiety, as a consequence of different torsion angles in subunit (O=)C–N–C–C(=O) including the nitrogen atoms from Gly1 and/or Gly2. Conformers with the **C** pattern hydrogen bond (also found in the crystal; see Figure 1) are also present.

Whereas the structures **A** without HBs are not significant for ester **3**, they are quite abundant in conjugate **4**, in which about half of the population contains this pattern. Conformers **4A1** and **4A2** differ mostly in the rotation angle around the (Cp)C–C(substituent) bond so that the first alanine methyl group points either towards or away from the other Cp. The forms **4B** and **4C**, geometrically very similar to their Gly analogues **3B** and **3C**, are also present.

The spectroscopic data for the conjugates **3** and **4** are fully consistent with the conformation preferences obtained by DFT calculations. The rejection of conformer **D** on the basis of the IR and NMR spectroscopy results agrees well with its high relative energy. The experimentally substantiated weak IHBs involving the NH_{AA2} group, assigned to **B**- and **C**-type conformers, are fully supported by the computational approach. Whereas for the Gly conjugate **3** these

Table 3. Relative energies of the most stable conformers in chloroform at 298 K (under 3 kJ mol^{-1}), pseudo-torsion angles (C–*Cg*–*Cg*–C) and selected NH···O distances in hydrogen bonds in ferrocenes **3**–**6**.

Type	Δ*E* [kJ mol^{-1}]	(C–*Cg*–*Cg*–C) [°] pseudo-torsion angle	*d*(NH···O) [Å] (interchain)	*d*(NH···O) [Å] (intrachain)
3B1	0.00	–	–	1.99
3C	0.71	–	–	2.33
3B1	0.98	–	–	2.00
4A1	0.00	–	–	–
4B	1.06	–	–	2.17
4A2	1.07	–	–	–
4C	1.25	–	–	2.28
5H1(1,1′)[a]	0.00	9.3	1.97	–
5H2(1,2′)	1.11	72.4	2.11	–
5H3(1,1′)	1.58	0.6	2.05	–
5H4(1,2′)	3.04	68.9	2.15	–
6H1(*P*-1,1′)	0.00	11.6	2.07	–
6E1(*P*-1,2′)	1.41	71.5	2.48[b]	–
6E2(*M*-1,5′)	1.49	–72.1	2.42[b]	–
6H2(*P*-1,1′)	2.48	1.2	1.98	–

[a] Only (*P*) forms of the four corresponding enantiomeric pairs of **H** are given. [b] *d*(CH···O) [Å].

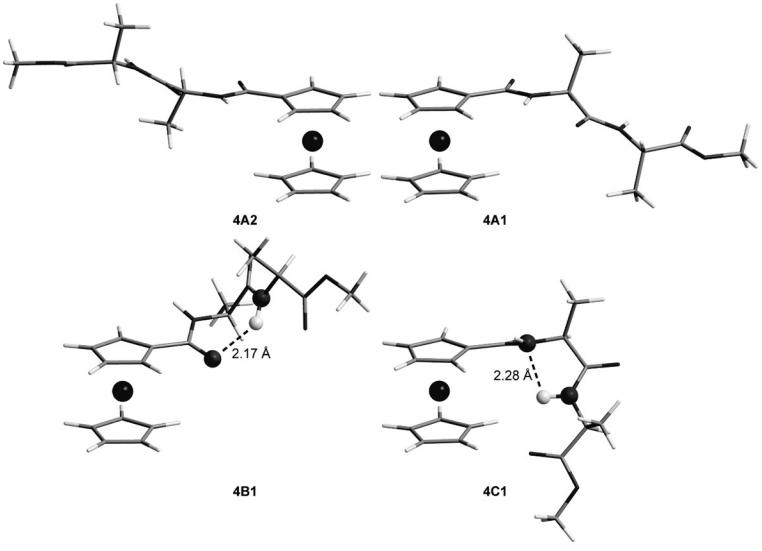

Figure 9. The most important types of conformers in alanine dipeptide **4** (Gly dipeptide **3** includes similar conformers of **B** and **C** types).

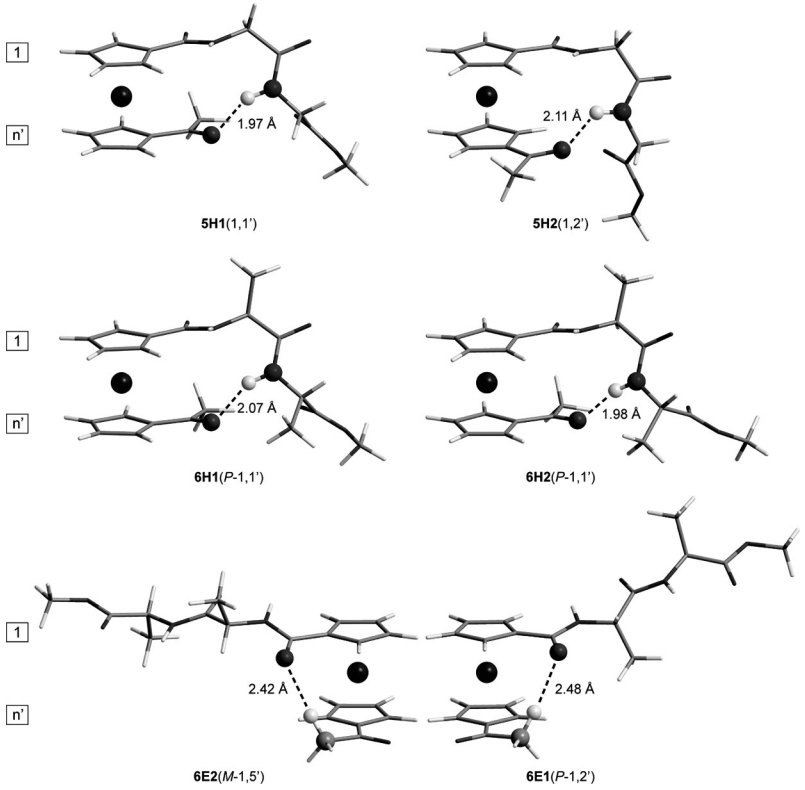

Figure 10. Top: the most stable types of **5H** pattern featuring 1,1′- and 1,2′-substitution modes [similar conformers **5H3** (1,1′) and **5H4** (1,2′) are omitted]. Bottom: ensemble of the most important forms of conjugate **6**.

conformers are the most stable ones, the ensemble of the most stable conformers for compound **4** also includes **4A**. These data and the absence of the **3A** forms can be explained in terms of the sterically more demanding alanine side chain's relative destabilization of intrastrand HBs of the **B** and **C** type.

The presence of a hydrogen-accepting 1′-acetyl substituent on the ferrocene unit increases the number of possible IHBs. In conjugates **5** and **6** one could expect more conformers (containing hydrogen bond patterns **E**–**J**; see Scheme 3) than in the model compounds **3** and **4**. Surprisingly, in the Gly dipeptide **5** only one IHB pattern dominates, with a 10-membered ring formed by spanning the 1′-Ac carbonyl and NH_{Gly2} groups. The resulting **H**-type conformers consist of four enantiomeric pairs **5H1**–**5H4** (e.g., configurations 1,2′/1,5′). For the sake of simplicity only the (*P*) forms (of two energetically equal counterparts) are depicted in Figure 10 and characterized in Table 3. The **5H1/5H3** conformers with 1,1′ geometry are generally more populated than those with 1,2′ configuration (**5H2/5H4**). These two sets differ mostly in their (O=)C–N–C–C(=O) torsion angles including nitrogen from Gly2.

In ester **6** in chloroform, two hydrogen bond patterns dominate. The geometry of the more stable conformer **6H1** with 1,1′-positioned substituents (pseudo-torsion angle ω = 11.6°) is similar to that of **5H1**. There is another (*P*) isomer adopting an almost eclipsed conformation (**6H2**, ω = 1.2°), but **6H1** has a lower energy due to the favourable nonbonding interaction between the closely positioned alanine ester and acetyl groups. The ensemble of the most populated conformers of **6** also includes two conformers (1,2′ **6E1** and 1,5′ **6E2**) of opposite ferrocene chirality and almost equal relative energies. These structures without NH···O hydrogen bonds are more stable than 1,3′ and 1,4′ isomers (so-called "Xu"-conformers[39]). One may note that vectors belonging to C=O groups directly attached to the Cp rings in conjugate **5** and **6** can point in the same or opposite (towards each other) directions. To describe these relationships, modified CIP rules in which stereochemical *E*/*Z* descriptors were assigned to the substituents were applied. Conventionally the first symbol refers to the top ring and the second to the bottom ring. [In such a way for any helical isomer – e.g., (*P*)-1,2′ – four geometrical isomers are hypothetically possible: *E*,*E*; *E*,*Z*; *Z*,*E* and *Z*,*Z*]. By applying this stereochemical nomenclature to conformers of **5** and **6** depicted in Figure 2, we can characterize all the (*P*)-1,1′ forms as *E*,*E* isomers, **5H2**(*P*)-1,2′ belongs to *E*,*Z* type, whereas both of the **6E** conformers are *Z*,*E* isomers.

Preliminary analysis with the aid of Bader's atoms in molecules (AIM) theory indicates interaction that can be described as a weak CH···O hydrogen bond forming a seven-membered ring with the proton-donating acetyl methyl group and the ferrocene-1-carbonyl oxygen as proton acceptor. The bond critical point (BCP) is observed between oxygen and proton. Topological properties [the electron density ρ(r), the Laplacian of the electron density $\nabla^2\rho$(r) and the energy density H(r) in a.u.] at this BCP have the following values: ρ(r) = 0.009, $\nabla^2\rho$(r) = 0.027, H(r) = 0.0008

for **6E1** and $\rho(r) = 0.010$, $\nabla^2\rho(r) = 0.030$, $H(r) = 0.0009$ for **6E2**. The values for the first two parameters are in the range of the criteria proposed by Popelier[40] for the existence of HB [i.e., 0.002–0.035 a.u. for $\rho(r)$ and 0.024–0.139 a.u. for $\nabla^2\rho(r)$]. If the second two parameters are considered [$\nabla^2\rho(r) > 0$ and $H(r) > 0$], as suggested by Rozas et al.,[41] the HB could be classified as a weak hydrogen bond.

As in the cases of conjugates **3** and **4**, calculations for their 1′-acetyl derivatives **5** and **6** also support the spectroscopic findings. Conformer **J** was ruled out on the basis of spectroscopic evidence similar to that described for its analogue **D**. The lowest-energy conformers of the Gly conjugate **5** include only the **H** pattern. The ensemble of the most stable conformers of the Ala conjugate **6** includes **6H** and conformers of the **6E** type without NH···O hydrogen bonds. This is reminiscent of the calculation results obtained for Gly conjugate **4**, for which similar patterns including NH_{Ala2} appear in **4B** and **4C**, together with **4A**. With the similar conformation distributions for **3** and **5** in mind, these relationships can be explained by the steric factors discussed above.

The CD spectra of the types **I**–**IV** containing chiral amino acids (Scheme 1) reflect ferrocene chirality. A positive Cotton effect in the region of about 470 nm means preponderance of (*P*)-helical ferrocene conformations over (*M*) arrangements and vice versa. On the basis of our calculation results one can see that (*P*) orientations in **6** contribute more than their (*M*) counterparts (Table 3), which fits nicely with the observed positive CD signal.

Conclusions

In continuation of our studies on "desymmetrized" conjugates of ferrocene-1,1′-dicarboxylic acid and amino acids/peptides (type **III**, Scheme 1) we have performed conformation analyses of compounds **5** and **6** ($n = 2$; X = OMe; Y = Me; R = H/Me) and their model substances Fc-CO-AA-AA-OMe (**3**, AA = Gly; **4**, AA = Ala) to address the question of individual conformation preferences in solution and to reveal their molecular structures in the solid state. In our previous research into similar conjugates (e.g., **III**, $n = 1$, X = Y = NHMe, R = H/Me/*i*Pr[21]) we found a multitude of conformations without preference for one specific conformer, in which an increase in the steric demand of the amino acid side chain reduced the number of conformations.

By means of X-ray analysis it was shown that self-assembly processes (including N–H···O, C–H···O hydrogen bonds and π···π interactions) prevailed in compound **5** in the solid state.

The thorough spectroscopic investigation of systems **3**–**6** in solution in nonpolar solvents (CH_2Cl_2, $CDCl_3$), and also in [D_6]DMSO, demonstrated the domination of intramolecular hydrogen-bonded NH_{AA2} forming intra- and interchain conformers, accompanied by open forms. In the model compounds **3** and **4**, NH_{AA2} was IHBd with FcCO (**B**, γ-turn), as well as with N_{AA1} to form the five-membered rings **C**. [It is worth mentioning that an analogous five-membered intrachain pattern was also found in conjugate **5** in the solid state.] On the basis of the IR and NMR data for dipeptides **5** and **6** (v.r. method, NMR titration, dilution experiments, etc.) negligible HB interactions of NH_{AA1} were demonstrated, whereas NH_{AA2} were included in medium/weak IHBs, which could result in the formation of **F** and **G** forms (reminiscent of **B** and **C**), as well as of interchain conformer **H**. Conformations **D** and **J** were rejected by IR analysis.

Systematic analysis of the conformation spaces of all of the studied compounds was conducted by combinations of molecular mechanics and B3LYP calculations, with implicit solvent effects included through the IEF-PCM method. Chloroform was used as the best approximation of experimental conditions. The calculation results corroborated the experimental findings for the monosubstituted compounds **3** and **4**, with the most stable conformers belonging to the **A**, **B** or **C** types. In analogous 1′-acetyl derivatives, only the **H** (for **5** and **6**) and **E** (for **6**) conformers are significantly populated. Whereas the Gly dipeptides **3** and **5** contain larger proportions of conformers with the hydrogen-donating NH_{AA2} group, the conformation distributions for the alanine dipeptides **4** and **6** are different. They also contain significant proportions of structures **A** and **E**. One can conclude that bulkier alanine side chain destabilizes conformations containing the overbridging NH_{AA2} group (**B**, **C** and **H** types).

DFT calculations for the chiral disubstituted molecule **6** showed the presence of fewer (*M*)- and more (*P*)-helical ferrocenes in the **H/E** ensemble, in accordance with the experimentally observed positive Cotton effect.

Finally, it can be concluded that the conformation distributions of conjugates **5** and **6**, in comparison with the above-mentioned MeNH-CO-Fn-CO-AA-NHMe,[21] are dramatically changed with the omission of only one hydrogen-donating substituent (1′-MeNH).

Experimental Section

General: The syntheses were carried out under argon. CH_2Cl_2 used for synthesis and FT-IR spectroscopy was dried (P_2O_5), distilled from CaH_2 and stored over molecular sieves (4 Å). Products were purified by preparative thin-layer chromatography on silica gel (Merck, Kieselgel 60 HF_{254}) with use of CH_2Cl_2/EtOAc mixtures as eluents. Melting points were determined with a Buechi apparatus. IR spectra were recorded as CH_2Cl_2 solutions and KBr pastilles with a Bomem MB 100 mid FT-IR spectrophotometer. ^1H and $^{13}C\{^1H\}$ NMR spectra were recorded with a Varian EM 360 or Varian Gemini 300 spectrometer in $CDCl_3$ and [D_6]DMSO solutions with Me_4Si as internal standard or with a Varian Unity Plus 400 spectrometer. CD spectra were recorded as CH_2Cl_2 solutions under argon with a Jasco-810 CD spectrophotometer in 1 cm quartz Suprasil cells. Ellipticity maxima (λ_{max}), are given in nm. Molar ellipticity coefficients (M_θ) were calculated as $M_\theta = 100\theta/c \times l$, where ellipticity ($\theta$) is in deg, concentration (c) in M and pathlength (1) in cm, thus giving deg M^{-1} cm^{-1} for M_θ.[42] Friedel–Crafts acetylation of *N*,*N*-diphenylferrocenecarboxamide gave its 1′-acetyl derivative, which was hydrolysed to 1′-acetylferrocene-1-

carboxylic acid (**2**).[26] The reference compounds **7/8** and **9/10** were prepared as described in the references.[24,43]

Preparation of Fc-CO-AA-AA-OMe (3 and 4) and MeCO-Fn-CO-AA-AA-OMe (5 and 6)

General Procedure: EDC (264 mg, 1.36 mmol) and HOBt (183 mg, 1.36 mmol) were added to a suspension of ferrocenecarboxylic acid (**1**) or keto acid **2** (1.10 mmol) in dry dichloromethane (10 mL) and the reaction mixture was stirred for 1 h at room temp. A solution of Boc-AA-AA-OCH_3 (380 mg, 1.5 mmol) in AcOEt was deprotected by treatment with gaseous HCl. H-AA-AA-OCH_3 hydrochloride resulting after evaporation of the solvent was treated with Et_3N in CH_2Cl_2 and added to a solution of activated **1** or **2**. The mixture was stirred for 1 h at room temperature and washed with saturated aqueous $NaHCO_3$ and water. The organic layer was dried with Na_2SO_4, concentrated in vacuo and TLC-purified with CH_2Cl_2/EtOAc (10:1) as eluent.

Compound 3 (AA = Gly): Yield 240 mg (51%), yellow crystals, m.p. 113–118 °C. ^{1}H NMR (300 MHz, $CDCl_3$, 25 °C): δ = 6.89 (t, J = 4.74 Hz, 1 H, NH_{Gly2}), 6.59 (t, J = 4.49 Hz, 1 H, NH_{Gly1}), 4.74 (t, 2 H, Cp-H), 4.38 (t, 2 H, Cp-H), 4.24 (s, 5 H, $Cp_{unsubst.}$), 4.13 (d, J = 5.49 Hz, 2 H, $CH_{2,Gly2}$), 4.10 (d, J = 5.40 Hz, 2 H, $CH_{2,Gly1}$), 3.76 (s, 3 H, $COOCH_3$) ppm. ^{1}H NMR (300 MHz, [D$_6$]DMSO, 25 °C): δ = 8.27 (t, J = 5.64 Hz, 1 H, NH_{Gly1}), 8.07 (t, J = 6.24 Hz, 1 H, NH_{Gly2}), 4.79 (t, 2 H, Cp-H), 4.35 (t, 2 H, Cp-H), 4.22 (s, 5 H, $Cp_{unsubst.}$), 3.90 (d, J = 5.89 Hz, 2 H, $CH_{2,Gly2}$), 3.84 (d, J = 5.70 Hz, 2 H, $CH_{2,Gly1}$), 3.63 (s, 3 H, $COOCH_3$) ppm. ^{13}C NMR, APT (300 MHz, $CDCl_3$, 25 °C): δ = 172.0 (s, $COOCH_3$), 170.7 (s, C=O), 169.7 (s, C=O), 78.66 (s, C-1, Fc), 71.6 (s, C-2, -5), 69.9 (s, C-3, -4), 70.1 (s, $Cp_{unsubst.}$), 53.0 (s, $COOCH_3$), 43.1 (s, $CH_{2,Gly2}$), 41.9 (s, $CH_{2,Gly1}$) ppm. $C_{16}H_{18}FeN_2O_4$ (358.18): calcd. C 53.65, H 5.06, N 7.82; found C 53.45, H 5.04, N 7.79.

Compound 4 (AA = Ala): Yield 295 mg (59%), orange crystals, m.p. 123–127 °C (124–126 °C).[24] ^{1}H NMR (300 MHz, $CDCl_3$, 25 °C): δ = 7.22 (d, J = 4.74 Hz, 1 H, NH_{Ala2}), 6.57 (d, J = 4.49 Hz, 1 H, NH_{Ala1}), 4.82 (m, 1 H, CH_{Ala2}), 4.75 (s, 2 H, Cp-H), 4.55 (m, 1 H, CH_{Ala1}), 4.35 (s, 2 H, Cp-H), 4.20 (s, 5 H, $Cp_{unsubst.}$), 3.75 (s, 3 H, $COOCH_3$), 1.50 (d, J = 6.80 Hz, 3 H, $CH_{3,Ala1}$), 1.44 (d, J = 7.1 Hz, 3 H, CH_{3Ala2}) ppm. ^{1}H NMR (300 MHz, [D$_6$]DMSO, 25 °C): δ = 8.28 (d, J = 6.28 Hz, 1 H, NH_{Ala2}), 7.71 (d, J = 7.7 Hz, 1 H, NH_{Ala1}), 4.90 (s, 1 H, Cp-H), 4.79 (s, 1 H, Cp-H), 4.46 (m, 1 H, CH_{Ala2}), 4.43 (m, 3 H, CH_{Ala1}, Cp-H), 4.18 (s, 5 H, $Cp_{unsubst.}$), 3.62 (s, 3 H, $COOCH_3$), 1.32 (d, J = 1.2 Hz, 3 H, $CH_{3,Ala1}$), 1.30 (d, J = 1.97 Hz, 3 H, $CH_{3,Ala2}$) ppm. ^{13}C NMR, APT (300 MHz, $CDCl_3$, 25 °C): δ = 172.6 (s, $COOCH_3$), 170.7 (s, C=O), 169.7 (s, C=O), 74.7 (s, C-1, Fc), 70.2 (s, C-2, -5), 69.7 (s, C-3, -4), 68.0 (s, $Cp_{unsubst.}$), 51.9 (s, $COOCH_3$), 48.1 (s, CH_{Ala2}), 48.0 (s, CH_{Ala1}), 18.3 (s, $CH_{3,Ala1}$), 17.3 (s, $CH_{3,Ala2}$) ppm. $C_{18}H_{22}FeN_2O_4$ (386.23): calcd. C 55.98, H 5.74, N 7.25; found C 55.77, H 5.73, N 7.23.

Compound 5 (AA = Gly): Yield 230 mg (53%), red-orange crystals, m.p. 109–112 °C. ^{1}H NMR (300 MHz, $CDCl_3$, 25 °C): δ = 7.54 (t, J = 5.13 Hz, 1 H, NH_{Gly2}), 7.01 (t, J = 5.46 Hz, 1 H, NH_{Gly1}), 4.81 (pt, 2 H, Cp-H), 4.77 (pt, 2 H, Cp-H), 4.58 (pt, 2 H, Cp-H), 4.40 (pt, 2 H, Cp-H), 4.10 (d, J = 5.50 Hz, 2 H, $CH_{2,Gly1}$), 4.08 (d, J = 5.40 Hz, 2 H, $CH_{2,Gly2}$), 3.73 (s, 3 H, $COOCH_3$), 2.37 (s, 3 H, $COCH_3$) ppm. ^{1}H NMR (300 MHz, [D$_6$]DMSO, 25 °C): δ = 8.29 (s, 1 H, NH_{Gly1}), 8.20 (s, 1 H, NH_{Gly2}), 4.82 (s, 2 H, Cp-H), 4.79 (s, 2 H, Cp-H), 4.60 (s, 2 H, Cp-H), 4.40 (s, 2 H, Cp-H), 3.89 (s, 2 H, $CH_{2,Gly1}$), 3.83 (s, 2 H, $CH_{2,Gly2}$), 3.62 (s, 3 H, $COOCH_3$), 2.30 (s, 3 H, $COCH_3$) ppm. ^{13}C NMR, APT (300 MHz, $CDCl_3$, 25 °C): δ = 202.9 (s, $COCH_3$), 17.4 (s, $COOCH_3$), 170.1 (s, C=O), 169.6 (s, C=O), 80.1 (s, C-1, Fc), 77.2 (s, C-6, Fc), 73.8 (s, C-2, -5), 71.9 (s, C-7, -10), 71.4 (s, C-3, -4), 70.2 (s, C-8, -9), 52.4 (s, $COOCH_3$), 43.4 (s, $CH_{2,Gly2}$), 41.2 (s, $CH_{2,Gly1}$), 27.7 (s, $COCH_3$) ppm. $C_{18}H_{20}FeN_2O_5$ (400.22): calcd. C 54.02, H 5.04, N 6.99; found C 53.81, H 5.02, N 7.01.

Compound 6 (AA = Ala): Yield 310 mg (67%), yellow-orange crystals, m.p. 125–130 °C. ^{1}H NMR (300 MHz, $CDCl_3$, 25 °C): δ = 7.14 (d, J = 7.02 Hz, 1 H, NH_{Ala2}), 6.61 (d, J = 7.02 Hz, 1 H, NH_{Ala1}), 4.79 (pt, 1 H, Cp-H), 4.73 (pt, 1 H, Cp-H), 4.68 (pt, 1 H, Cp-H), 4.66 (m, 1 H, CH_{Ala1}), 4.63 (pt, 1 H, Cp-H), 4.54 (m, 1 H, CH_{Ala2}), 4.52 (pt, 1 H, Cp-H), 4.50 (pt, 1 H, Cp-H), 4.34 (pt, 2 H, Cp-H), 3.72 (s, 3 H, $COOCH_3$), 2.36 (s, 3 H, $COCH_3$), 1.48 (d, J = 7.02 Hz, 3 H, $CH_{3,Ala1}$), 1.40 (d, J = 7.02 Hz, 3 H, CH_{3Ala2}) ppm. ^{1}H NMR (300 MHz, [D$_6$]DMSO, 25 °C): δ = 8.29 (d, J = 7.02 Hz, 1 H, NH_{Ala2}), 7.80 (d, J = 7.02 Hz, 1 H, NH_{Ala1}), 4.93 (s, 1 H, Cp-H), 4.81 (s, 1 H, Cp-H), 4.76 (s, 2 H, Cp-H), 4.56 (s, 2 H, Cp-H), 4.40 (m, 1 H, CH_{Ala1}), 4.39 (s, 2 H, Cp-H), 4.27 (m, 1 H, CH_{Ala2}), 3.61 (s, 3 H, $COOCH_3$), 2.36 (s, 3 H, $COCH_3$), 1.31 (d, J = 7.02 Hz, 3 H, $CH_{3,Ala1}$), 1.30 (d, J = 7.02 Hz, 3 H, CH_{3Ala2}) ppm. ^{13}C NMR, APT (300 MHz, $CDCl_3$, 25 °C): δ = 209.9 (s, $COCH_3$), 172.4 (s, $COOCH_3$), 171.1 (s, C=O), 168.6 (s, C=O), 79.7 (s, C-1, Fc), 76.9 (s, C-6, Fc), 73.8 (s, C-2, Fc), 73.2 (s, C-5, Fc), 71.5 (s, C-7, Fc), 71.4 (s, C-10, Fc), 70.9 (s, C-3, Fc), 70.8 (s, C-4, Fc), 69.7 (s, C-8, Fc), 69.5 (s, C-9, Fc), 51.9 (s, $COOCH_3$), 48.4 (s, CH_{Ala2}), 47.2 (s, CH_{Ala1}), 27.2 (s, $COCH_3$), 18.0 (s, $CH_{3,Ala1}$), 17.5 (s, $CH_{3,Ala2}$) ppm. $C_{20}H_{24}FeN_2O_5$ (428.27): calcd. C 56.09, H 5.65, N 6.54; found C 55.87, H 5.63, N 6.50.

X-ray Determination of 5: A single crystal of **5** suitable for X-ray single crystal analysis was obtained at room temperature by partial evaporation from a dichloromethane solution. An orange prismatic crystal, with dimensions $0.31 \times 0.36 \times 0.47$ mm^3, was selected for X-ray structure analysis. The intensities were collected at 295 K with an Oxford Diffraction Xcalibur2 diffractometer and use of graphite-monochromated Mo-K_α radiation (λ = 0.71073 Å). *CrysAlis*[44] programs were used for data collection and reduction. The intensities were corrected for absorption by use of the multi-scan absorption correction method (*CrysAlis RED*;[44] T_{min} = 0.85912/T_{max} = 1.00000). The crystal structure was solved by direct methods.[44] All non-hydrogen atoms were refined anisotropically by full-matrix, least-squares calculations based on F^2.[45] The hydrogen atoms of the N1 and N2 atoms were found in a difference Fourier map and their coordinates and isotropic thermal parameters were refined freely. All other hydrogen atoms were included in calculated positions as riding atoms, with *SHELXL97*[45] defaults. The *PLATON*[46] program was used for structure analysis and drawings preparation.

CCDC-733644 contains the supplementary crystallographic data for this paper. These data can be obtained free of charge from The Cambridge Crystallographic Data Centre via www.ccdc.cam.ac.uk/data_request/cif.

Crystal Data: $C_{18}H_{20}FeN_2O_5$, M_r = 400.21, monoclinic space group $P2_1/c$ (No. 14); a = 7.1210(6), b = 22.8830(17), c = 10.5532(11) Å, β = 99.869(8)°, V = 1694.2(3) Å^3; Z = 4; $D_{calcd.}$ = 1.569 g cm^{-3}; μ(Mo-K_α) = 0.923 mm^{-1}; R_{int} = 0.0187; S = 0.994; R/wR = 0.0332/0.0925 for 245 parameters and 4378 reflections with $I \geq 2\sigma(I)$, R/wR = 0.0395/0.0977 for all 4915 independent reflections in the range 7.76° – 2θ – 60.00°.

DMSO Titrations of 5 and 6: Compound **5** or **6** (approximately 20 mg) was dissolved in $CDCl_3$ (500 μL) in an NMR sample tube. A measured amount of [D$_6$]DMSO was added to the NMR tube by micropipette and the mixture was then inverted several times to ensure good homogeneity. This procedure was repeated for successive additions of [D$_6$]DMSO until the percentage of DMSO reached 40% (by volume).

Computational Details: Starting geometries for DFT optimizations of compounds **3**–**6** were generated by full conformation space search by use of the MacroModel v9.5[47] molecular modelling program with several different search methods and force fields. Details of the procedure will be published in a forthcoming paper.[22b]

All of the obtained conformers were then fully optimized at the B3LYP/LanL2DZ[48] level of theory, and the most stable of them were reoptimized in chloroform with use of the B3LYP method and the 6-311G(d,p) basis set for all atoms except for Fe, for which the ECP set LanL2DZ was used. The IEF-PCM method implemented in Gaussian was used for describing implicit solvent effects. All quantum-mechanical calculations were performed with Gaussian03vE1,[49] and graphical representations of optimized structures were prepared with the help of GaussView[50] and Chem3D (CambridgeSoft, Cambridge, MA). The topological analysis of the selected ferrocenes was performed with AIM2000 program.[51]

Supporting Information (see also the footnote on the first page of this article): Selected bond lengths, bond and torsion angles for **5**; hydrogen-bonding geometry for **5**. CD spectra of **6** in KBr disk.

Acknowledgments

This research was supported by the Ministry of Science, Education and Sports of the Republic of Croatia (grant Nos. 058-1191344-3122, 119-1193079-3069 and 119-1191342-1339.)

[1] a) Throughout the text Fc denotes ferrocenyl and Fn means ferrocene-1,1′-diyl (the alternative designation of this substituent by fc[1b] is confusing because of its resemblance to Fc); b) P. Stepnicka, *Ferrocenes: Ligands, Materials and Biomolecules*, John Wiley & Sons, **2008**.
[2] H.-A. Klok, *Angew. Chem. Int. Ed.* **2002**, *41*, 1509–1513.
[3] D. Kanamori, T. Okamura, H. Yamamoto, N. Ueyama, *Angew. Chem. Int. Ed.* **2005**, *44*, 969–972.
[4] D. J. Hill, M. J. Mio, R. B. Prince, T. S. Hughes, J. S. Moore, *Chem. Rev.* **2001**, *101*, 3893–4011.
[5] I. Huc, *Eur. J. Org. Chem.* **2004**, 17–29.
[6] E. R. Kay, D. A. Leigh, F. Zerbetto, *Angew. Chem. Int. Ed.* **2007**, *46*, 72–191.
[7] T. Moriuchi, T. Hirao, *Chem. Soc. Rev.* **2004**, *33*, 294–301.
[8] D. R. van Staveren, N. Metzler-Nolte, *Chem. Rev.* **2004**, *104*, 5931–5985.
[9] a) S. Chowdhury, G. Schatte, H.-B. Kraatz, *Angew. Chem.* **2008**, *120*, 7164–7167; *Angew. Chem. Int. Ed.* **2008**, *47*, 7056–7059; b) S. Chowdhury, D. A. R. Sanders, G. Schatte, H.-B. Kraatz, *Angew. Chem.* **2006**, *118*, 765–768; *Angew. Chem. Int. Ed.* **2006**, *45*, 751–754.
[10] T. Moriuchi, T. Nagai, T. Hirao, *Org. Lett.* **2005**, *7*, 5265–5268.
[11] S. I. Kirin, D. Wissenbach, N. Metzler-Nolte, *New J. Chem.* **2005**, *29*, 1168–1173.
[12] S. Chowdhury, G. Schatte, H.-B. Kraatz, *Dalton Trans.* **2004**, 1726–1730.
[13] F. E. Appoh, T. C. Sutherland, H.-B. Kraatz, *J. Organomet. Chem.* **2004**, *689*, 4669–4677.
[14] T. Moriuchi, K. Yoshida, T. Hirao, *Org. Lett.* **2003**, *5*,4285–4288.
[15] T. Moriuchi, A. Nomoto, K. Yoshida, T. Hirao, *Organometallics* **2001**, *20*, 1008–1013.
[16] T. Moriuchi, A. Nomoto, K. Yoshida, A. Ogawa, T. Hirao, *J. Am. Chem. Soc.* **2001**, *123*, 68–75.
[17] T. Moriuchi, A. Nomoto, K. Yoshida, T. Hirao, *J. Organomet. Chem.* **1999**, *589*, 50–58.
[18] A. Nomoto, T. Moriuchi, S. Yamazaki, A. Ogawa, T. Hirao, *Chem. Commun.* **1998**, 1963–1964.
[19] R. S. Herrick, R. M. Jarret, T. P. Curran, D. R. Dragoli, M. B. Flaherty, S. E. Lindyberg, R. A. Slate, L. C. Thornton, *Tetrahedron Lett.* **1996**, *37*, 5289–5292.
[20] S. Chowdhury, K. A. Mahmoud, G. Schatte, H.-B. Kraatz, *Org. Biomol. Chem.* **2005**, *3*, 3018–3023.
[21] J. Lapić, D. Siebler, K. Heinze, V. Rapić, *Eur. J. Inorg. Chem.* **2007**, 2014–2024.
[22] a) J. Lapić, *Dissertation*, University of Zagreb, Zagreb, **2008**; b) J. Lapić, I. Kodrin, Z. Mihalić, V. Rapić, manuscript in preparation.
[23] S. Djakovic, D. Siebler, M. Čakić Semenčic, K. Heinze, V. Rapic, *Organometallics* **2008**, *27*, 1447–1453.
[24] L. Barišić, M. Čakić, K. A. Mahmoud, Y.-n. Liu, H.-B. Kraatz, H. Pritzkow, S. I. Kirin, N. Metzler-Nolte, V. Rapić, *Chem. Eur. J.* **2006**, *12*, 4965–4980.
[25] V. Kovač, K. Radolović, I. Habuš, D. Siebler, K. Heinze, V. Rapić, *Eur. J. Inorg. Chem.* **2009**, 389–399.
[26] W. F. Little, R. Eisenthal, *J. Am. Chem. Soc.* **1960**, *82*, 1577–1580.
[27] J. Bernstein, R. E. Davis, L. Shimoni, N.-L. Chang, *Angew. Chem. Int. Ed. Engl.* **1995**, *34*, 1555–1573.
[28] L. Barišić, M. Dropučić, V. Rapić, H. Pritzkow, S. I. Kirin, N. Metzler-Nolte, *Chem. Commun.* **2004**, 2004–2005.
[29] D. R. van Staveren, T. Weyhermüller, N. Metzler-Nolte, *Dalton Trans.* **2003**, 210–220.
[30] X. de Hatten, T. Weyhermüller, N. Metzler-Nolte, *J. Organomet. Chem.* **2004**, *689*, 4856–4867.
[31] S. I. Kirin, U. Schatzschneider, X. de Hatten, T. Weyhermuller, N. Metzler-Nolte, *J. Organomet. Chem.* **2006**, *691*, 3451–3457.
[32] L. Lin, A. Berces, H.-B. Kraatz, *J. Organomet. Chem.* **1998**, *556*, 11–20.
[33] C. A. Hunter, J. K. M. Sanders, *J. Am. Chem. Soc.* **1990**, *112*, 5525–5534.
[34] W. Bauer, K. Polborn, W. Beck, *J. Organomet. Chem.* **1999**, *579*, 269–279.
[35] J. Lapić, G. Pavlović, D. Siebler, K. Heinze, V. Rapić, *Organometallics* **2008**, *27*, 726–735.
[36] S. I. Kirin, H.-B. Kraatz, N. Metzler-Nolte, *Chem. Soc. Rev.* **2006**, *35*, 348–354.
[37] T. P. Curran, A. B. Lesser, R. S. H. Yoon, *J. Organomet. Chem.* **2007**, *692*, 1243–1254, and references cited therein.
[38] K. Heinze, M. Beckmann, *Eur. J. Inorg. Chem.* **2005**, 3450–3457.
[39] Y. Xu, P. Saweczko, H.-B. Kraatz, *J. Organomet. Chem.* **2001**, *335*, 637–639.
[40] a) U. Koch, P. L. A. Popelier, *J. Phys. Chem.* **1995**, *99*, 9747–9754; b) P. L. A. Popelier, *J. Phys. Chem. A* **1999**, *102*, 1873–1878.
[41] I. Rozas, I. Alkorta, J. Elguero, *J. Am. Chem. Soc.* **2000**, *122*, 11154–11161.
[42] S. M. Kelly, T. J. Jess, N. C. Price, *Biochim. Biophys. Acta* **2005**, *1751*, 119–139.
[43] Y. Jin, K. Tonan, S. Ikawa, *Spectrochim. Acta Part A* **2002**, *58*, 2795–2802.
[44] Oxford Diffraction, Xcalibur CCD System, *CrysAlis CCD* and *CrysAlis RED*, versions 1.171.31.5, Oxford Diffraction, Oxford, United Kingdom, **2006**.
[45] G. M. Sheldrick, *Acta Crystallogr., Sect. A* **2008**, *64*, 112–122.
[46] A. L. Spek, *J. Appl. Crystallogr.* **2003**, *36*, 7–13.
[47] a) *MacroModel*, version 9.5, Schrodinger, LLC, New York, NY, **2007**; b) F. Mohamadi, N. G. J. Richards, W. C. Guida, R. Liskamp, M. Lipton, C. Caufield, G. Chang, T. Henrickson, W. C. Still, *J. Comput. Chem.* **1990**, *11*, 440–467.
[48] a) D. Becke, *J. Chem. Phys.* **1993**, *98*, 5648–5652; b) C. Lee, W. Yang, R. G. Parr, *Phys. Rev. B* **1998**, *37*, 785–789.
[49] M. J. Frisch, G. W. Trucks, H. B. Schlegel, G. E. Scuseria, M. A. Robb, J. R. Cheeseman, J. A. Montgomery Jr., T. Vreven, K. N. Kudin, J. C. Burant, J. M. Millam, S. S. Iyengar, J. Tomasi, V. Barone, B. Mennucci, M. Cossi, G. Scalmani, N. Rega, G. A. Petersson, H. Nakatsuji, M. Hada, M. Ehara, K.

Toyota, R. Fukuda, J. Hasegawa, M. Ishida, T. Nakajima, Y. Honda, O. Kitao, H. Nakai, M. Klene, X. Li, J. E. Knox, H. P. Hratchian, J. B. Cross, V. Bakken, C. Adamo, J. Jaramillo, R. Gomperts, R. E. Stratmann, O. Yazyev, A. J. Austin, R. Cammi, C. Pomelli, J. W. Ochterski, P. Y. Ayala, K. Morokuma, G. A. Voth, P. Salvador, J. J. Dannenberg, V. G. Zakrzewski, S. Dapprich, A. D. Daniels, M. C. Strain, O. Farkas, D. K. Malick, A. D. Rabuck, K. Raghavachari, J. B. Foresman, J. V. Ortiz, Q. Cui, A. G. Baboul, S. Clifford, J. Cioslowski, B. B. Stefanov, G. Liu, A. Liashenko, P. Piskorz, I. Komaromi, R. L. Martin, D. J. Fox, T. Keith, M. A. Al-Laham, C. Y. Peng, A. Nanayakkara, M. Challacombe, P. M. W. Gill, B. Johnson, W. Chen, M. W. Wong, C. Gonzalez, J. A. Pople, *Gaussian 03*, revision E.01, Gaussian, Inc., Wallingford CT, 2004.

[50] *GaussView*, version 4.1, Roy Dennington, II, Todd Keith and John Millam, Semichem, Inc., Shawnee Mission, KS, **2007**.

[51] a) F. Biegler-König, J. Schömbohm, D. J. Bayles, *J. Comp. Chem.* **2001**, *22*, 545–559; b) F. Biegler-König, J. Schönbohm, *J. Comp. Chem.* **2002**, *23*, 1489–1494.

Received: December 9, 2009
Published Online: March 18, 2010

